ELSEVIER

MCN Molecular and Cellular Neuroscience

www.elsevier.com/locate/ymcne
Mol. Cell. Neurosci. 30 (2005) 465 – 475

Cortistatin overexpression in transgenic mice produces deficits in synaptic plasticity and learning

Melanie K. Tallent,[a] Véronique Fabre,[b,1] Cuie Qiu,[a] Marta Calbet,[b] Tyra Lamp,[c] Michael V. Baratta,[c] Chisa Suzuki,[b] Coree L. Levy, [c] George R. Siggins,[c] Steven J. Henriksen,[c] José R. Criado,[c] Amanda Roberts,[c] and Luis de Lecea [b,c,*]

[a]*Department of Pharmacology and Physiology, Drexel University, University College of Medicine, Philadelphia, PA 19102, USA*
[b]*Department of Molecular Biology, The Scripps Research Institute, La Jolla, CA 92037, USA*
[c]*Department of Neuropharmacology, The Scripps Research Institute, La Jolla, CA 92037, USA*

Received 4 March 2005; revised 18 July 2005; accepted 17 August 2005
Available online 22 September 2005

Cortistatin-14 (CST) is a neuropeptide expressed in cortical and hippocampal interneurons that shares 11 of 14 residues with somatostatin. In contrast to somatostatin, infusion of CST decreases locomotor activity and selectively enhances slow wave sleep. Here, we show that transgenic mice that overexpress cortistatin under the control of neuron-specific enolase promoter do not express long-term potentiation in the dentate gyrus. This blockade of dentate LTP correlates with profound impairment of hippocampal-dependent spatial learning. Exogenously applied CST to slices of wild-type mice also blocked induction of LTP in the dentate gyrus. Our findings implicate cortistatin in the modulation of synaptic plasticity and cognitive function. Thus, increases in hippocampal cortistatin expression during aging could have an impact on age-related cognitive deficits.

Introduction

Cortistatin-14 (CST) is a recently described neuropeptide of the somatostatin family (de Lecea et al., 1996). Preprocortistatin mRNA is primarily expressed in a subset of cortical and hippocampal GABAergic interneurons, which partially colocalize with somatostatin-positive cells (de Lecea et al., 1997a). The mature cortistatin peptide shares 11 of its 14 amino acid residues with somatostatin and binds in vitro to the five somatostatin receptors (sst1-5) with similar affinity as somatostatin (de Lecea et al., 1996; Criado et al., 1999; Fukusumi et al., 1997; Siehler et al., 1998). A new human orphan receptor MgrX2 has recently been shown to selectively bind cortistatin-17 with high affinity (Robas et al., 2003), suggesting that there may be cortistatin-specific signaling pathways.

Application of CST in vitro to hippocampal slices hyperpolarizes hippocampal CA1 pyramidal neurons and enhances the M-current (de Lecea et al., 1996), as has been described for SST (Moore et al., 1988). However, CST also has distinct actions from SST in vitro in augmenting the H-current in CA1 pyramidal neurons (Schweitzer et al., 2003), supporting the idea that it has distinct mechanisms. Likewise, CST has distinct effects when applied in vivo. Intracerebroventricular administration of synthetic CST reduces locomotor activity and selectively enhances slow-wave sleep (de Lecea et al., 1996). Also, CST antagonizes the effects of acetylcholine on cortical and hippocampal excitability (de Lecea et al., 1996), in contrast to somatostatin, which is known to enhance acetylcholine responses (Mancillas et al., 1986).

The electrophysiological properties of CST suggest that the peptide may exert other functions, in addition to its sleep promoting activity. In particular, the interactions of CST with acetylcholine suggest that it may have an effect on learning and memory (Hasselmo, 1999; Hasselmo and Barkai, 1995; Aigner, 1995). Consistent with this hypothesis, intracerebroventricular injection of CST in rats impairs memory in two different tasks (Flood et al., 1997; Sanchez-Alavez et al., 2000).

To learn more about the effects of endogenous cortistatin peptide in hippocampal function, we have generated transgenic mice that overexpress preprocortistatin in postmitotic neurons.

Here, we show that overexpression of cortistatin in these mice has dramatic consequences in the plasticity of the dentate gyrus which correlate with impairment of hippocampal-dependent forms of learning.

* Corresponding author. Department of Molecular Biology, MB-10, The Scripps Research Institute, 10550 North Torrey Pines Road, La Jolla, CA 92037, USA. Fax: +1 858 784 9120.
E-mail address: llecea@scripps.edu (L. de Lecea).
[1] Present address: INSERM U288, Faculté de Médecine Pitié-Salpêtrière, 75634 Paris.
Available online on ScienceDirect (www.sciencedirect.com).

1044-7431/$ - see front matter © 2005 Elsevier Inc. All rights reserved.
doi:10.1016/j.mcn.2005.08.010

Results

Cortistatin overexpressing mice

We generated transgenic mice harboring a construct containing the neuron-specific enolase (NSE) promoter (Forss-Petter et al., 1990) fused to the mouse preprocortistatin cDNA (de Lecea et al., 1997b) (Fig. 1A). From 14 transgenic founders, five transmitted the transgene to their offspring and three transgenic lines were positive for expression of the transgene, with varying levels of expression. Transgenic lines 22 and 69 showed transgene expression throughout the brain, although line 69 had the highest mRNA concentrations of preprocortistatin (Fig. 1B). Preprocortistatin in wild-type mice is expressed exclusively in GABAergic interneurons throughout the cortex and in the CA1–CA3 fields (Fig. 1C). No preprocortistatin positive cells can be detected in the dentate gyrus of wild-type mice, consistent with previous results (Fig. 1E) (de Lecea et al., 1997a,b). In contrast, expression of preprocortistatin in transgenic line 69 was localized in the pyramidal cell layer of all hippocampal fields, as well as granule cells and hilar neurons in the dentate gyrus (Fig. 1F). Strong levels of expression were also detected in pyramidal and nonpyramidal cells throughout the cerebral cortex, and reticular thalamus (Fig. 1D). Transgenic mice were viable and fertile and showed no overt behavioral abnormalities. Line 22 showed moderate transgenic expression in the dentate gyrus and CA1 region (not shown). We performed test electrophysiological experiments in lines 22 and 69. The effect of transgene expression on dentate gyrus LTP appeared dose-dependent. Line 22 showed attenuation of dentate gyrus LTP, whereas line 69 showed a complete blockade of LTP (see below). Therefore, line 69 was chosen for further analysis.

In vitro electrophysiological studies

Cortistatin blocks dentate LTP

We tested the effects of cortistatin expression in the dentate gyrus by looking at the amplitude of the evoked responses after stimulation of the perforant path. We measured population spike and fEPSP amplitudes in dentate granule cells in both transgenic and wild-type littermates from the three different transgenic lines.

Synaptic responses to different stimulus intensities were the same in CST transgenic as in wild-type mice (Fig. 2A). The initial slope of the fEPSP in wild-type mice was 0.12 ± 0.01, 0.28 ± 0.04, and 0.49 ± 0.05 mV/ms measured at threshold, half-maximal and maximal stimulus intensities, respectively (n = 18). In CST transgenics the fEPSP initial slope was 0.13 ± 0.02, 0.31 ± 0.03, and 0.48 ± 0.06 mV/ms measured at threshold, half-maximal, and maximal stimulus intensities, respectively (n = 11). There was no statistical significance in the values between the two groups ($P >$ 0.5). We also examined paired-pulse facilitation of the fEPSP at three different interstimulus intervals (15, 30, 50, and 100 ms). Paired-pulse facilitation was modestly attenuated in the CST transgenics compared to controls (Fig. 2B). At an interstimulus interval of 30 and 50 ms, the paired-pulse ratio was significantly different between control and transgenic ($P < 0.05$).

We next examined the ability of the perforant path/dentate granule cell synapses to undergo LTP after high-frequency trains (HFTs). LTP at this synapse was greatly compromised in the CST tgs compared to wild-type (Fig. 3A; $P < 0.0005$). Significant potentiation (>10%) was present in only 1 of 8 slices from transgenic mice. 60 min following the train the fEPSP slope in transgenics was 86 ± 12% of the baseline slope. In slices from wild-types (n = 13), 60 min following the trains, the fEPSP slopes were 134 ± 8% of baseline. In addition, short-term potentiation (STP) 1–5 min following the trains was also greatly attenuated relative to control ($P < 0.0005$). In the slices from the transgenics, mean fEPSP slope 1 min after the trains was 141 ± 15% of baseline. In slices from wild-type animals, mean fEPSP slope 1 min following the train was 215 ± 21% of baseline. From 1–5 min following the train, STP was significantly depressed in CST transgenics compared to wild-type ($P < 0.5$).

To determine whether exogenous CST had an inhibitory effect on dentate LTP, we applied the peptide (1 μM) to slices from C57Bl/6J mice, for 7 min prior to giving HFTs, and washed it out 1 min later. At 60 min following HFT, significant potentiation was generated in only 3 of 11 slices. With CST application, the mean

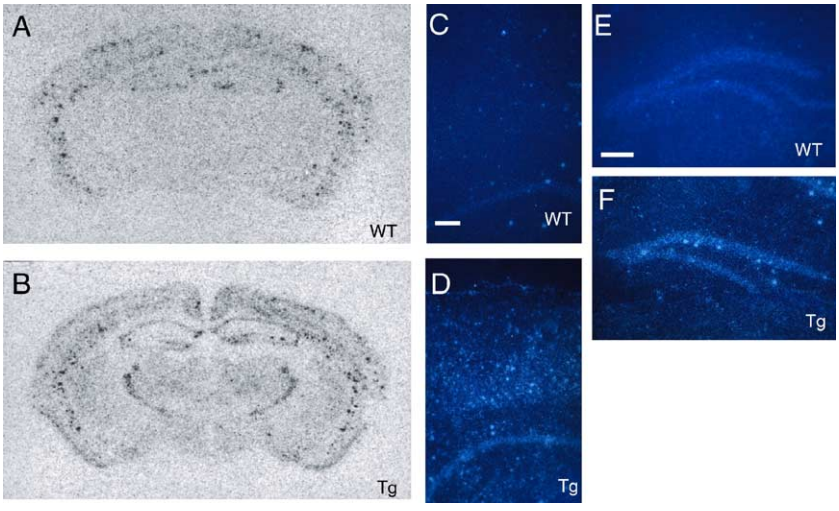

Fig. 1. Transgenic mice overexpressing preprocortistatin. (A) In situ hybridization of a section of a wild-type mouse hybridized with a preprocortistatin riboprobe. (B) Coronal section of an in situ hybridization to mouse preprocortistatin in a transgenic animal from line 69. Note high levels of transgene expression in the cerebral cortex, hippocampal formation, and reticular thalamus. Dark field micrographs of the in situ hybridization to preprocortistatin in the neocortex (C, D) and dentate gyrus (E, F) of wild-type (C, E), and transgenic (D, F) mice. Scale bar, 250 μm.

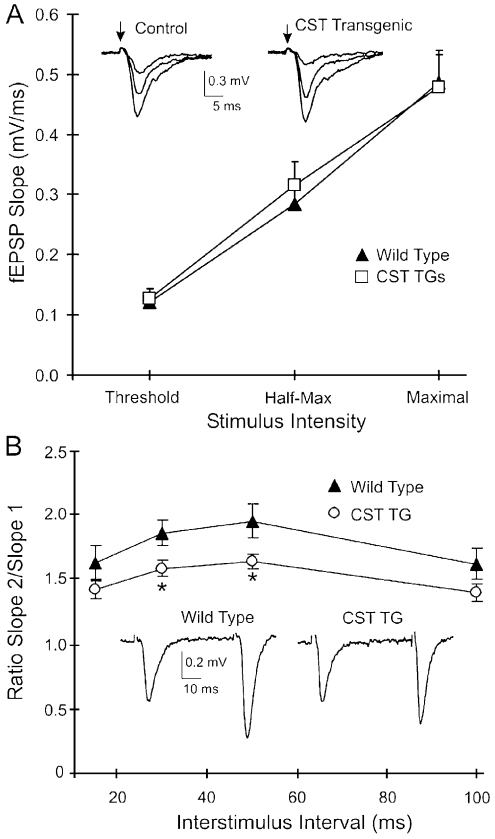

Fig. 2. Synaptic function at lateral perforant path synapses in CST transgenics (CST TGs). (A) Synaptic response to stimulation of lateral perforant path fibers is similar in wild-type ($n = 18$) and CST transgenics ($n = 11$). Input–output response is evoked at different stimulus intensities and measured as initial slope of the field EPSP (mV/ms). Inset: representative fEPSPs evoked at half-maximal stimulus intensities for wild-type and CST transgenics. (B) Reduction in paired-pulse facilitation in CST transgenics. Synaptic response to pairs of stimuli is measured as the ratio of the slope of the second fEPSP to the first fEPSP. Facilitation of the second fEPSP is reduced at 30 and 50 ms interstimulus intervals (asterisk, $P < 0.05$) in CST transgenics ($n = 14$) compared to wild-types ($n = 10$). Inset: representative responses to a pair of stimuli with a 30 ms interstimulus interval for wild-type and CST transgenics.

fEPSP slope 60 min following HFTs was 95.0 ± 10% of baseline (Fig. 3B), which was significantly reduced from wild-type ($n = 15$; $P < 0.0005$) and not different from baseline ($P > 0.05$), indicating that no LTP was generated. STP was slightly but significantly reduced as well ($P < 0.005$). In contrast, when we superfused CST for 15 min beginning 30 min after the induction of LTP, no significant effect of CST was seen ($n = 7$). After 15 min of CST application (45 min after HFTs), fEPSP slope was 144 ± 6% of baseline. At the same time in control slices, the fEPSP slope was 144 ± 8% of baseline ($n = 13$). At 60 min following HFTs, in slices where CST had been applied, fEPSP slopes were 132 ± 9% of baseline, compared to 139 ± 6% in control slices. No significant differences in LTP were found between the two groups. Thus, after LTP has been induced, CST does not affect its maintenance.

CA1 LTP is expressed in CST transgenics

We next examined CA1 synaptic responses in the CST transgenic mice. No difference between wild-type ($n = 9$) and CST transgenics ($n = 7$) was seen in input–output responses to Schaeffer collateral stimulation (Fig. 4A) or paired-pulse facilitation ($n = 4–6$). In contrast to dentate, consistent LTP is observed in CA1 of the CST overexpressing animals (Fig. 4A; $n = 9$). At 60 min post-HFT, initial slope of the fEPSP is 185 ± 8% of baseline. In slices from wild-type mice ($n = 9$), fEPSP slope was 213 ± 20% of baseline 60 min after the trains. Thus, although consistent, robust LTP can be generated in CST transgenic mice, the amplitude of LTP is significantly less (25%) than in wild-type mice ($P < 0.0005$). STP was also compromised in the CST transgenics; the mean initial slope 1 min following HFTs was 208 ± 22% of baseline (Fig. 4A). In wild-type slices, mean initial slope 1 min after trains was 287 ± 30% of baseline. Overall, for the first 5 min following the trains, STP was significantly less in slices from CST transgenics ($P < 0.05$).

Likewise, exogenous application of CST results in less robust depression of LTP in CA1 compared to dentate. Application of 1 μM CST significantly reduced the degree of CA1 potentiation (Fig. 4B; $n = 7$). Unlike in dentate, however, LTP was not completely blocked. Slope of the fEPSP 60 min following the train was significantly enhanced after CST application compared to baseline ($P < 0.05$). At 60 min following the trains, the initial slope was 191 ± 17% of control in the absence of CST ($n = 9$). When CST was applied prior to and during the trains, potentiation was reduced to 145 ± 8% of control. This represents a 50% reduction in the degree of potentiation.

In vivo electrophysiological studies

We characterized neuronal excitability, local circuit interactions and synaptic plasticity in CST tg mice in vivo by generating input/output curves, paired-pulse responses, and LTP in the dentate gyrus. Stimulation of the perforant path generated evoked field-potentials recorded in the gyrus. The waveforms consisted of a fast negative-going PS superimposed on the field EPSP/IPSP (data not shown). The excitability of dentate granule neurons in transgenic mice overexpressing CST was not different from their wild-type littermates at any stimulus level (Fig. 5A; ANOVA; $P > 0.05$). We next examined the effects of CST overexpression in paired-pulse responses in the dentate gyrus. Equipotent paired orthodromic stimulation of the perforant path in wild-type mice elicited a triphasic test/conditioning response curve. Transgenic lines overexpressing CST 69 had a longer period of early inhibition that were significantly different from wild-type mice at 40 and 60 ms (Fig. 5B; ANOVA; $P < 0.05$). We then determined the ability to generate LTP in the dentate gyrus in vivo. HFTs of the perforant path in wild-type mice produced a marked and prolonged increase in dentate PS amplitudes. HFTs of the perforant path in transgenic mice from line 69 overexpressing CST produced a marked and prolonged reduction in PS amplitudes (Fig. 5C; ANOVA; $F_{2,18} = 20.81$, $P < 0.0001$).

Behavioral analysis of cortistatin overexpressing mice

Lack of hippocampal LTP is associated with deficits in spatial memory (Tsien et al., 1996). To determine the behavioral consequences of cortistatin-induced blockade of LTP in the dentate gyrus, we analyzed the performance of transgenic mice in the hippocampal-dependent spatial Barnes maze test. Three additional tests were performed to examine behaviors which potentially could influence performance in this particular learning task. These included general locomotion (locomotor activity test), anxiety

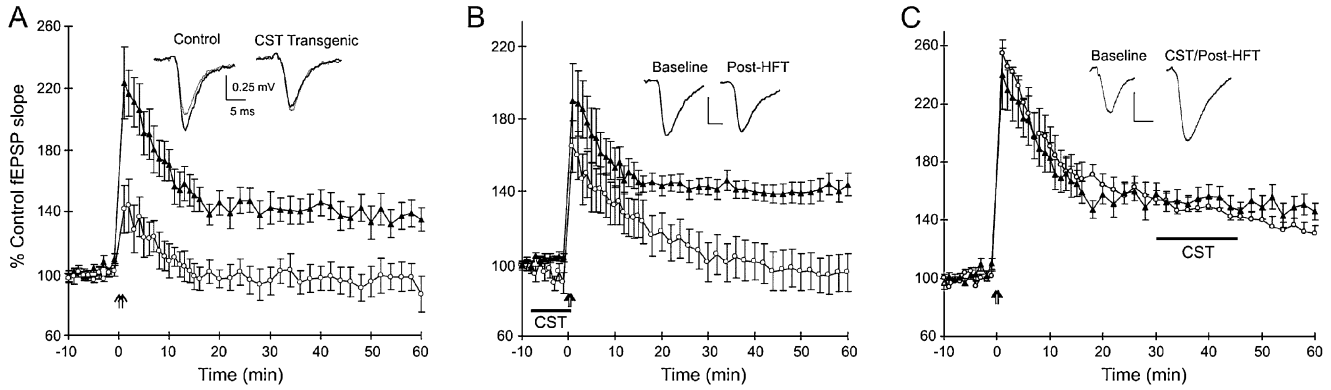

Fig. 3. Dentate gyrus LTP is greatly compromised in CST transgenic mice. (A) Mean data from control and CST transgenic slices. Initial slope is plotted over time 10 min prior to 60 min following high-frequency trains (double arrows). Reduced short-term potentiation and no long-term potentiation are seen in CST transgenics (open circles; $n = 8$) relative to controls (filled triangles; $n = 13$). Inset: representative fEPSPs from a control and a transgenic mouse before (gray) and 60 min following two 1 s 100 Hz trains (black). No potentiation of the fEPSP is seen in slices from dentate of the CST transgenic mouse. Scale bar labels are the same for all subsequent traces. (B) Exogenous CST also reduces LTP. CST (1 μM; open circles) was superfused beginning 7 min prior to HFTs for a total of 8 min (black bar). A small decrease in the fEPSP slope was observed prior to HFTs (maximal inhibition was 11 ± 4% 7 min following the beginning of the superfusion). No significant potentiation is present 60 min following the trains when CST was superfused during the induction protocol (control, $n = 13$; CST, $n = 11$). Inset: representative fEPSPs before and 60 min following HFTs with CST superfusion. (C) Exogenous CST does not affect LTP maintenance. 1 μM CST was applied from 30–45 min (black bar) following HFTs (open circles; $n = 7$). No significant effect on magnitude of LTP was observed compared to control slices ($n = 13$). Inset: representative baseline and 60 min posttrain fEPSP from experiment where CST was applied 30–45 min following train.

(light/dark transfer test), and visual acuity (visual cliff test). There were no significant differences between CST transgenic and wild-type mice in either locomotor activity (males: $F_{1,9} = 0.43$, N.S.; females: $F_{1,12} = 0.02$, N.S.; Fig. 6A) or rearing behavior (males: $F_{1,9} = 0.66$, N.S.; females: $F_{1,12} = 0.59$, N.S.; not shown). An analysis of the first 22 sessions (those sessions prior to mice being removed that had reached the criteria for learning the task) revealed no significant difference between genotypes in number of holes visited in males ($F_{1,21} = 0.04$, $P = 0.8$). Female transgenic mice actually visited significantly more holes than WT mice ($F_{1,21} = 5.9$, $P < 0.05$), suggesting that they moved around the maze more than WT mice. Both sexes and genotypes showed a typical drop in activity as they habituated to the testing environment. The results indicate that overexpression of CST is not associated with a change in locomotor behavior. In addition, there were no significant differences between CST transgenic and wild-type mice in either the time spent in the light compartment (males: $t = -0.07$, N.S.; females: $t = 0.13$, N.S.) or the number of transitions between the light and dark compartments (males: $t = -0.37$, N.S.; females: $t = -0.83$, N.S.; Fig. 6B). Thus, it may be concluded that overexpression of CST is not associated with alterations in innate anxiety-like behavior. In the visual cliff test, both CST overexpressing and wild-type mice stepped down onto the safe side more than 50% of the time ($P < 0.05$; Fig. 6C), indicating that both genotypes have intact visual perception.

In contrast, spatial learning of NSE CST transgenic mice was severely impaired, compared with wild-type littermates (Fig. 7). A significantly greater proportion of wild-type mice reached the criterion for this test by day 40 relative to transgenic mice (males: χ^2 (1) = 7.6, $P < 0.01$; females: χ^2 (1) = 4.6, $P < 0.05$). In fact, none of the CST overexpressing males learned this task. The results from the behavioral experiments indicate that mice overexpressing

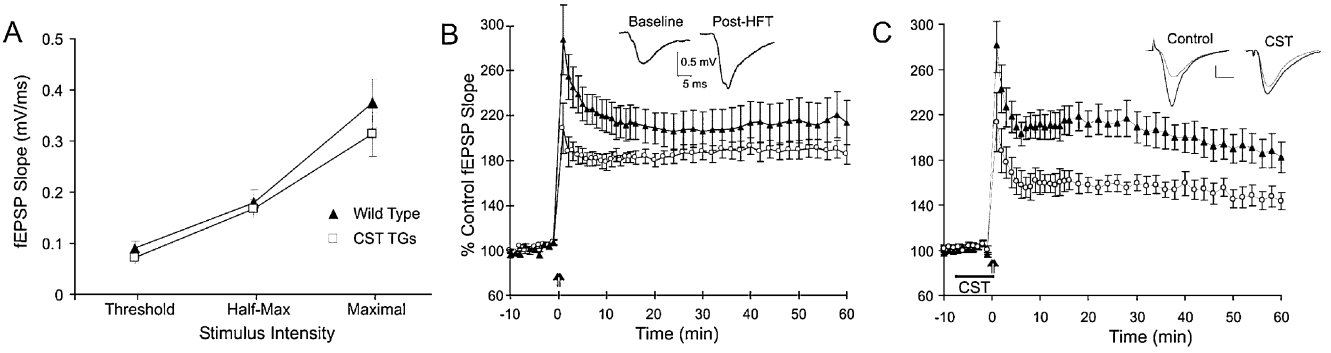

Fig. 4. CA1 LTP can be evoked in CST transgenics. Schaeffer collateral-evoked EPSPs were recorded in the stratum radiatum; mean data are plotted as for dentate. (A) No difference in stimulus-strength/synaptic response relationship is observed between wild-type ($n = 9$) and CST transgenics ($n = 7$). (B) Although significant LTP is generated in the CST transgenics (open circles; $n = 9$), a small but significant reduction in LTP and especially in STP is observed compared to nontransgenics (filled triangles; $n = 9$). Inset: recordings from a CST transgenics showing that CA1 LTP is still present 60 min following HFTs. (C) Cortistatin (1 μM; $n = 7$) significantly reduces but does not block LTP at CA1 synapses. CST was applied 7 min prior to and washed out 1 min following HFTs. Inset: left traces show baseline (gray) and potentiated (black) responses measured 60 min following train with no peptide application (control). Right traces are representative traces from an experiment where CST was applied before and during trains. Note the reduction in potentiation compared to control.

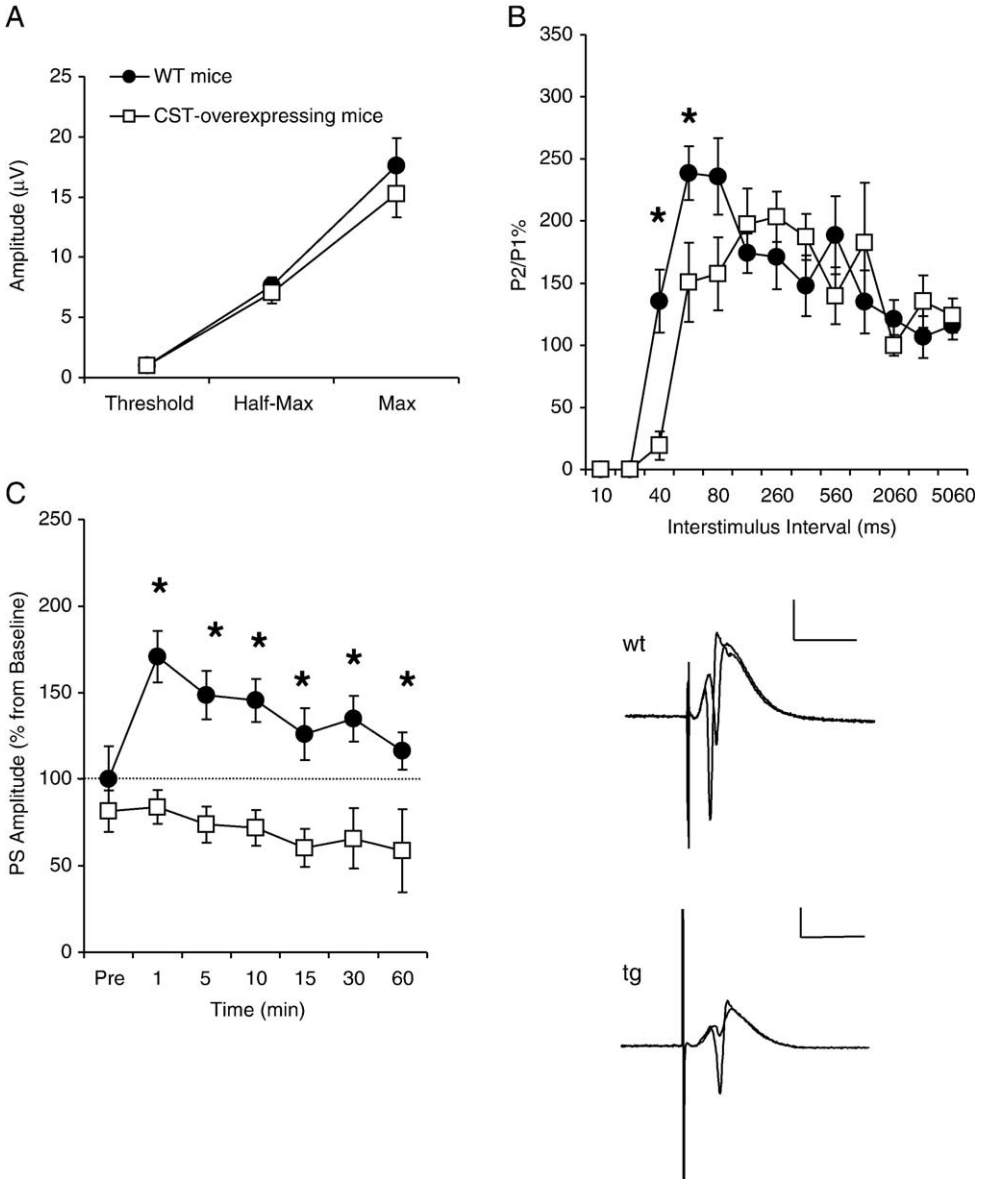

Fig. 5. Consequences of CST expression on dentate gyrus physiology in vivo. (A) Stimulation of the perforant path generated evoked field-potentials recorded in the gyrus. Values from CST-overexpressing mice and wild-type littermates were not significantly different at any stimulus level ($P > 0.05$). (B) Stimulation of the perforant path in wild-type mice was characterized by an early period of inhibition that lasted for 20 ms. Transgenic mice from line 69 had a longer period of early inhibition that were significantly different from wild-type mice at 40 and 60 ms ($n = 5$). Representative recordings of wave forms evoked in the dentate gyrus by perforant path stimulation (50% maximum) from a wild-type and transgenic mouse, 40 ms. Calibration 20 ms 1 mV (2). (C) High-frequency stimulation (HFS) of the perforant path in wild-type mice produced a marked and prolonged increase in dentate PS amplitudes termed, long-term potentiation (LTP). HFS of the perforant path in transgenic mice overexpressing CST produced a significant reduction in PS amplitudes ($n = 5$). Asterisks represent significance levels of $P < 0.05$ (ANOVA).

CST have severe defects in hippocampal-dependent long-term memory in the absence of alterations in locomotor activity, anxiety-like behavior and visual acuity.

Discussion

In the present study, we have generated transgenic mice expressing cortistatin in mature postmitotic neurons under the control of neuron-specific enolase promoter. In situ hybridization showed substantial concentrations of cortistatin mRNA expression throughout the cerebral cortex and pyramidal layer of the hippocampus and granule cells in the dentate gyrus as well as different extracortical regions including the thalamus. Transgenic line 22 showed lower levels of transgene expression and similar effects on paired-pulse inhibition than those observed with line 69. However, we could only observe attenuation of LTP in this transgenic line, suggesting a gene dosage effect. Since CST binding distribution overlaps with the distribution of somatostatin receptors in the cortex, amygdala, and hippocampus (Spier et al., 2005), overexpression of cortistatin in extracortical areas is unlikely to cause severe disruptions of neuronal activity.

Consistent with previous work (de Lecea et al., 1996), we have demonstrated that cortistatin has inhibitory activity in the hippo-

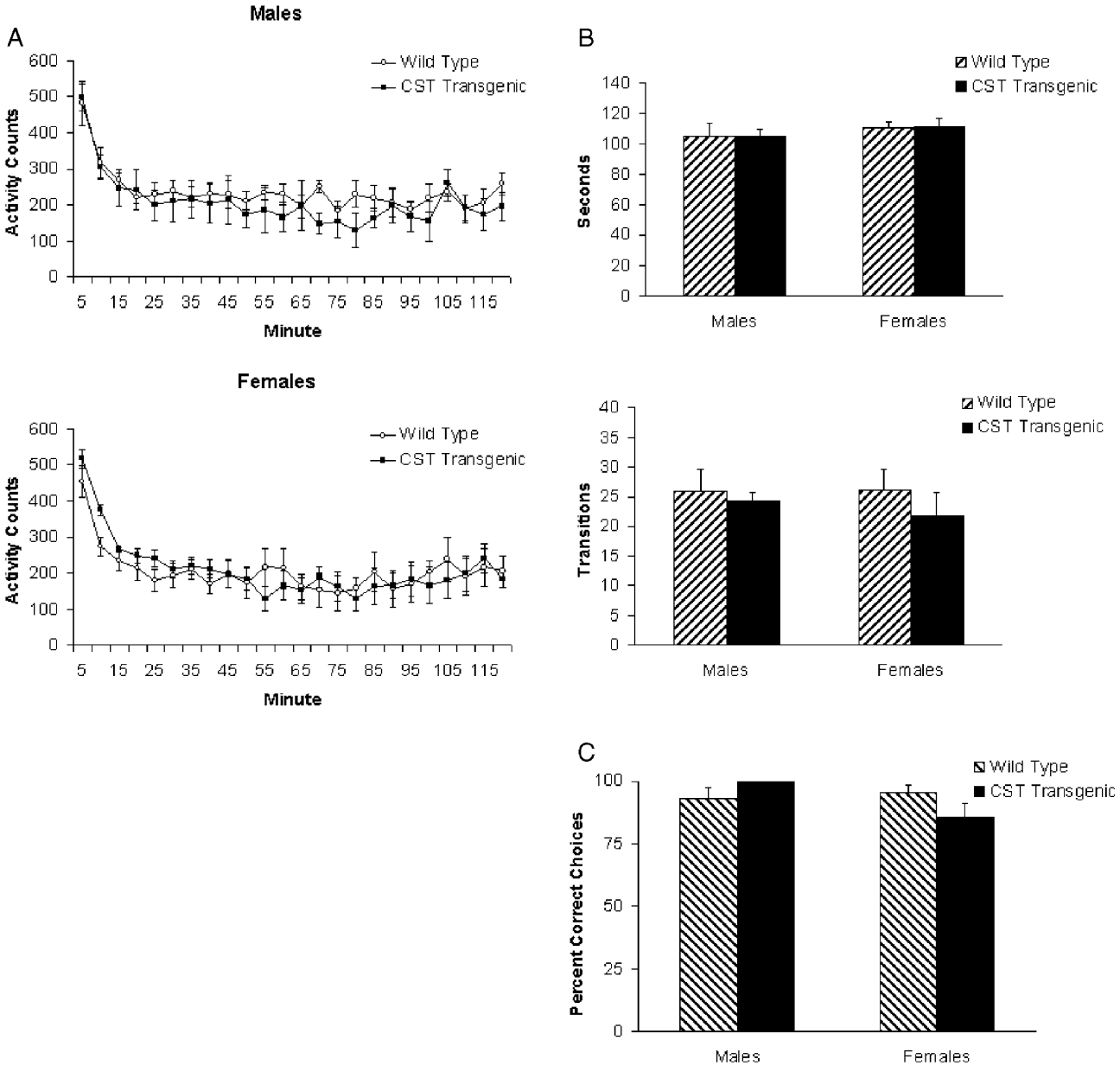

Fig. 6. NSE CST mice do not differ from wild-type mice in several general behavioral tests. (A) Locomotor activity of male (top) and female (bottom) wild-type and CST transgenic mice across a 2 h test period (n = 15). (B) Light/dark transfer behavior as determined by the time (seconds) spent in the light chamber (top) and the number of transitions between the dark and light compartments (bottom) in male and female wild-type and CST transgenic mice (n = 15). (C) Visual cliff data showing the percent of correct step down choices in male and female wild-type and CST transgenic mice (n = 15). All data are presented as means ± SEM. There were no significant effects of genotype in any of these behavioral measures.

campus. We found that dentate LTP recorded in vivo was disrupted in CST transgenics from line 69 and significantly attenuated in line 22. In hippocampal slices from CST transgenics, we also found that lateral perforant path LTP could not be induced. CA1 LTP, on the other hand, could still be expressed but was moderately attenuated. Similarly, exogenous application of synthetic CST blocks induction of long-term potentiation in dentate slices, as we have previously reported for SST (Baratta et al., 2002). However, CST did not block (although it reduced) induction of LTP in the CA1 region. The difference in the response to dentate and CA1 LTP could be because preprocortistatin mRNA is expressed at low levels in the dentate gyrus of wild-type mice (de Lecea et al., 1997a). Transgenic expression (or pharmacological application) to the dentate gyrus may inhibit synaptic transmission through interactions with somatostatin receptors, which are expressed in the dentate molecular layer (Videau et al., 2003). In contrast, endogenous expression of preprocortistatin is relatively high in CA1 of wild-type mice and does not appear to differ substantially in transgenic animals. These results therefore suggest that major alterations in hippocampal plasticity are restricted to areas with transgenic expression of CST. CA1 LTP is also less sensitive than dentate LTP to application of exogenous CST. This is similar to our finding with SST (Baratta et al., 2002; Qiu et al., 2003), suggesting that these two peptides

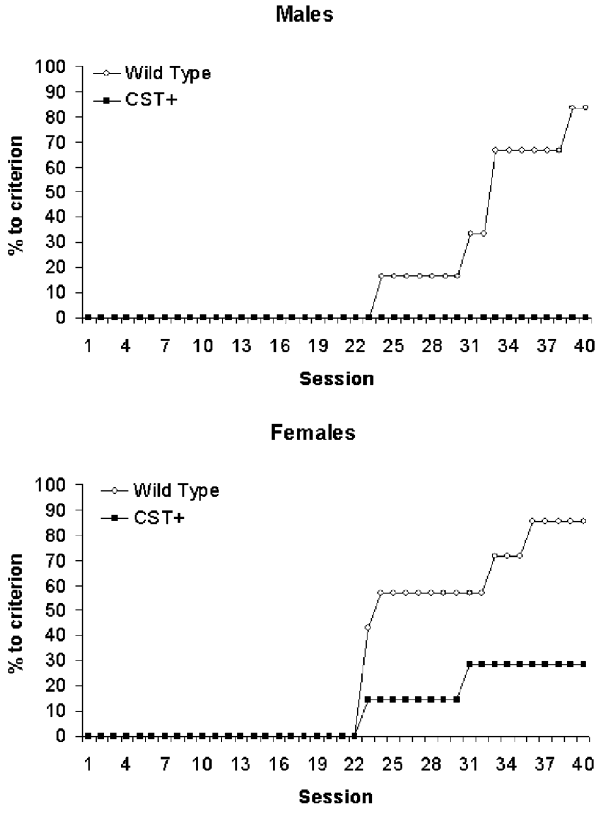

Fig. 7. NSE CST mice display impaired learning in the hippocampal-dependent Barnes maze task. The percent of mice in each group of males (top; $n = 10$) and females (bottom; $n = 10$) meeting the criterion for learning in this task (three errors or less on 7 of 8 consecutive trials) across the 40 days of testing. Both male and female CST transgenic mice showed impairment in this task as determined by significantly fewer mice in these groups learning this task (males: χ^2 (1) = 7.6, $P < 0.01$; females: χ^2 (1) = 4.6, $P < 0.05$).

may be acting through similar mechanisms to mediate their actions on hippocampal LTP.

LTP of both perforant path/granule cell synapses (Moser et al., 1998; Nakao et al., 2001) and Schaeffer collateral/CA1 synapses(Tsien et al., 1996) has been implicated in spatial learning. Our results support the conclusion that LTP in dentate may be more directly linked to spatial learning than CA1 LTP. However, since CA1 LTP, although present, was modestly reduced in CST transgenics, we cannot rule out that the spatial learning deficits were due to hypofunctional plasticity in CA1.

In view of the role of NMDA receptors in hippocampal LTP (Davis et al., 1992; Morris et al., 1986; Sakimura et al., 1995; Tsien et al., 1996), our findings could suggest an interaction between CST and NMDA receptor function. NMDA receptor-dependent LTP in the dentate gyrus appears to contribute to spatial learning (Moser et al., 1998). Our previous studies suggest that modulation by SST of postsynaptic Ca^+ entry through N-type Ca^+ channels is involved in inhibition of LTP by this peptide (Baratta et al., 2002). The reduction in STP, which is also a Ca^+- and NMDA receptor-dependent process (Anwyl et al., 1988; Malenka, 1991; McGuinness et al., 1991), by exogenous CST and in the CST transgenics also suggests that either of these two mechanisms may be involved. Further research is needed to determine whether the attenuation in dentate LTP is due to abnormal NMDA receptor function or a reduction of Ca^+ entry during the high-frequency trains.

The consequence of cortistatin overexpression on short-term plasticity was studied in both in vitro and in vivo anesthetized preparations. Our in vitro data suggest that CST transgenic and wild-type mice showed only modest differences in paired-pulse facilitation. In contrast, studies in vivo showed that, in comparison to wild-type mice, paired-pulse inhibition in CST transgenic mice was significantly reduced. These results may be attributed to differences in the electrophysiological preparations. Subcortical and cortical pathways that are known to modulate dentate function (e.g., septum) are intact in the in vivo preparation and may be also altered as a consequence of cortistatin overexpression.

It is becoming increasingly clear that inhibitory neuropeptides play a critical role in learning (for a recent review see Baraban and Tallent, 2004). For example, mice with the ORL1-receptor knocked-out show marked enhancement in learning spatial tasks and a corresponding increase in CA1 LTP (Manabe et al., 1998). Like CST, nociceptin also inhibits LTP in the dentate gyrus, although, unlike CST, this peptide also reduces the amplitude of baseline synaptic responses (Yu and Xie, 1998). The physiological relevance of neuropeptide modulation of synaptic plasticity and learning is yet unclear. High-frequency firing of interneurons, sufficient to release neuropeptides, occurs during normal exploratory activity in rodents. Other neuropeptide-containing interneurons, such as the alveus-oriens interneurons that express SST and CST, do not normally fire at a sufficiently high frequency to release neuropeptides (presumably ~25 Hz; Sun et al., 2003). However, cholinergic input increases the ability of these neurons to fire at high frequency (Jones and Yakel, 1997; Lawrence et al., 2003) and thus may facilitate release of neuropeptides. Hilar interneurons are also activated by cholinergic input (Frazier et al., 2003). Since CST inhibits cholinergic effects in hippocampus (de Lecea et al., 1996), cholinergic activation of CSTergic interneurons could comprise an inhibitory feedback mechanism. A possible function of CST in learning would be to increase the threshold for salient cues, thus acting to filter out distracting information.

Our results showing impaired spatial memory in the transgenic mice are also consistent with decreased cholinergic excitation in cortical structures. Cognitive decline during aging and in Alzheimer's disease has been associated to the loss of cholinergic neurons in the basal forebrain and decreased cholinergic tone in cortical structures. Upregulation of cortistatin mRNA observed in the dentate gyrus of aged mice may thus contribute to age-related decreases in cholinergic tone and cognitive deficits (Winsky-Sommerer et al., 2004). Intracerebroventricular injection of CST impairs posttraining memory processing (Sanchez-Alavez et al., 2000). The failure to obtain LTP in the dentate of CST transgenic mice correlates with severe deficits in the performance of spatial tasks such as the Barnes maze. The impairment of spatial memory is likely due to the inhibition of the entorhino-hippocampal perforant path, which is compromised during aging (Rosenzweig and Barnes, 2003). A possible function of CST in learning would be to increase the threshold for salient cues, thus acting to filter out distracting information.

Several recent studies have highlighted the relevance of sleep for memory consolidation (Louie and Wilson, 2001; Wilson and McNaughton, 1994) and cortical plasticity (Frank et al., 2001). In particular, the activity of several types of GABAergic interneurons, innervating different domains of the principal cells (axo axonic, chandelier, and oriens interneurons), appears to be dependent of the

brain state (Klausberger et al., 2003). LTP is inhibited during slow wave sleep (Leonard et al., 1987). Expression of cortistatin is regulated across the light–dark cycle and is increased upon sleep deprivation (Fabre et al., in preparation). Thus, it is possible that release of cortistatin at sleep onset promotes cortical synchronization and inhibits general plastic phenomena. Recent studies have shown that sleep deprivation dramatically inhibits the plastic phenomena in the visual cortex that accompany monocular deprivation during the critical period (Frank et al., 2001). In contrast, slow-wave sleep, during which cortistatin levels are low, enhances the area in the visual cortex that responds to both eyes, following monocular deprivation (Frank et al., 2001). Expression of preprocortistatin in the cortex inversely correlates with the changes of cortical plasticity that are affected by sleep. Moreover, low acetylcholine concentration during slow wave sleep, which may be attained by increased levels of cortistatin, has recently been shown to be critical for declarative memory consolidation (Gais and Born, 2004). Cortistatin may thus be a factor that contributes to the modulation of cortical plasticity and memory consolidation during sleep.

In sum, we have shown that transgenic expression and pharmacological application of CST inhibits long-term potentiation in vitro and in vivo. Our results are consistent with previous findings showing impairment of long-term memory in rats injected with CST (Sanchez-Alavez et al., 2000). Together, our findings implicate cortistatin in the modulation of synaptic plasticity and spatial learning, and suggest a role for this peptide in age-related cognitive deficits (Winsky-Sommerer et al., 2004).

Experimental methods

Cortistatin overexpressor mice

The cDNA encoding mouse preprocortistatin was digested with *Kpn*I and *Sma*I to insert a synthetic oligonucleotide as a transgenic tag 5′aac cga aca aaa act tat ttc tga aga aga tct g3′. A plasmid containing the NSE promoter fused to lacZ (Forss-Petter et al., 1990), was digested with *Hin*dIII and *Bam*HI to remove the beta galactosidase gene. The tagged preprocortistatin cDNA was inserted into the *Hin*dIII/*Bam*HI site of pNSE. The transgenic unit NSE-CST was injected into C57xSJL mouse oocytes as described (Forss-Petter et al., 1990). Transgenic mice were diagnosed by slot blot, using an SV40 polyA fragment as a probe, or by PCR. We backcrossed all transgenic lines for at least 7 generations into C57BL/6J background. All transgenic mice used in this study were hemizygous.

In situ hybridization

We conducted in situ hybridization essentially as described (de Lecea et al., 1997a). Briefly, we anesthetized young (3 months old) NSE:CST and aged matched wild-type littermates ($n = 5$) and aged wild-type mice (>26 month old C57BL6 J mice; $n = 4$) with halothane and perfused them intracardially with 4% paraformaldehyde in PBS pH 7.4 (PF). We removed the brains, postfixed them in the same fixative overnight, and cryoprotected them in sucrose dissolved in 4% PF-PBS. We collected 25 μm thick frozen sections in cryoprotectant solution (30% glycerol, 30% ethylene glycol 0.1 M PBS). We incubated free floating sections in 0.1% Triton in PBS, deproteinized with 0.2 N HCl for 10 min, acetylated with acetic anhydride (0.25% in 0.1 M triethanolamine hydrochloride pH 8) for 10 min, postfixed in 4%PF PBS for 10 min, and prehybridized at 55°C for 3 h in a solution containing 0.02 M PIPES, 10% (w/v) dextran sulfate, 50% formamide, 5× Denhardt's, 50 mM DTT, 2% SDS, 250 μg/ml yeast RNA, and 250 μg/ml denatured salmon sperm DNA. We labeled a cortistatin riboprobe by in vitro transcription of a 128 bp fragment (nucleotides 310–438) encoding mouse cortistatin using T3 RNA polymerase (Ambion) and ^{35}S UTP (NEN Dupont). A full length rat somatostatin cDNA was linearized and labeled with T7 RNA polymerase. We added labeled antisense cRNA to the sections (2×10^7 cpm/ml) and incubated overnight at 55°C. Sections were transferred to new vials and washed with 2 × SSC, 10 mM -mercaptoethanol (-ME) (30 min at room temperature), digested with RNAse A (37°C, 1 h), washed again with 1 × SSC, 50% formamide, 5 mM -ME (2 h at 55°C), and with 0.1× SSC (1 h, 68°C). We mounted sections on coated slides (Fisher) and exposed them to X-ray film and later to Ilford K5 autoradiographic emulsion for 4 weeks at 4°C. We developed the slides with Kodak D19 and counterstained with Richardson's blue. A sense cortistatin cRNA probe, transcribed with T7 RNA polymerase, was included as a negative control for most hybridization experiments.

In vitro electrophysiology

All studies were performed blind using either CST transgenic mice, originally on a C57/SJL background, backcrossed to C57BL/6J (N7), nontransgenic littermate, or C57BL/6J mice. As no difference was seen in the latter two groups, these results were pooled (wild-type group).

We prepared mouse hippocampal slices as described previously (Baratta et al., 2002). Briefly, male or female mice (6–14 weeks) were anesthetized with halothane (4%), decapitated, and the brains rapidly removed and placed in ice-cold artificial cerebrospinal fluid (ACSF), gassed with 95% O_2/5% CO_2 (carbogen), of the following composition (in mM): NaCl 130; KCl 3.5; NaH_2PO_4 1.25; $MgSO_4 7H_2O$ 1.5; $CaCl_2 2H_2O$ 2; $NaHCO_3$ 24; glucose 10. We cut transverse (for CA1) or horizontal (for dentate) brain slices (400 μM) using a Campden vibraslicer or a Vibratome Series 3000 (Technical Products International, St. Louis, MO). Hippocampal formations and adjacent entorhinal cortex (for dentate) were dissected from the slices and incubated in the recording chamber with their upper surfaces exposed to warmed, humidified carbogen, the slices were completely submerged and continuously superfused with gassed ACSF (31°C) at a constant rate (2–3 ml/min) for the remainder of the experiment. The inner chamber had a total volume of 1 ml; at the superfusion rates used, 90% replacement of the chamber solution could be obtained within 1–1.5 min. Drugs and peptides were added to the bath from stock solutions at known concentrations. We obtained CST from Peninsula Laboratories (San Carlos, CA). All other chemicals were from Sigma (St. Louis, MO).

Extracellular recording

We acquired data with an Axoclamp 2B amplifier (Axon Instruments) by D/A sampling using pCLAMP acquisition software (Axon Instruments). Extracellular field excitatory postsynaptic potentials (fEPSPs) were recorded in the outer molecular layer (OML) of the inner blade of the dentate using a glass micropipette filled with 3 M NaCl. We evoked perforant path synaptic responses at 0.033 Hz with a bipolar tungsten stimulating electrode placed near the apex of the dentate in the OML (Fig. 2A). Stable baseline

fEPSPs were confirmed by stimulating at 40–50% maximal field amplitude for 20–30 min prior to beginning experiments. For experiments in CA1, we placed a stimulating electrode in the stratum radiatum (SR) to stimulate Schaeffer collaterals, and recorded orthodromic fEPSPs in stratum radiatum.

We generated LTP with two high-frequency trains (HFTs) of 1 s each at 100 Hz, 20 s apart, using the maximal stimulus intensity for dentate and half-maximal for CA1. Test responses at 40–50% of maximal amplitudes were acquired for 15 min prior to and 60 min following trains. The mean initial slopes (between the 0 and 50% points on the rising phase) of 2–4 averaged fEPSPs were compared between the slice groups over the 60 min following LTP generation. To study effect on LTP induction, CST (1 μM) was added to the bath 7 min prior to, and washed out 1 min following, HFTs. For studies of LTP maintenance, CST was applied 30–45 min following HFTs.

In vivo electrophysiology

Mice were anesthetized with halothane (3–4%) and placed into a stereotaxic apparatus (Kopf Instruments; Tujunga, CA). Halothane anesthesia was adjusted to 0.8–1% following surgery and maintained at that level throughout the recording period. We measured population spike (PS) amplitudes and peak PS latencies from waveforms evoked in the dentate gyrus by stimulation of the angular bundle of the perforant path (coordinates: 3.6 mm posterior and 2.8 mm lateral relative to bregma; 2.0–2.5 mm ventral from dura) (Paxinos and Watson, 1986) with insulated, bipolar stainless steel electrodes (130 μm; 0.4–1.5 mA; 0.10 ms duration; average frequency, 0.1 Hz). Single barrel pipettes stereotaxically oriented into the ipsilateral dentate gyrus (coordinates: 2.0 mm posterior and 1.5 mm lateral relative to bregma; 1.8–2.5 mm ventral from dura) (Franklin and Paxinos, 1997) recorded extracellular evoked field potentials. Pipettes (2–3 μm, 3–20 MΩ) were filled with 0.5 M Na^+ acetate in 2% pontamine sky blue. PS amplitudes were recorded at multiple stimulus intensities and resultant input/output curves generated. Paired-pulses (PP) were delivered at 0.1 Hz and 3 responses were averaged at each interpulse interval. We generated LTP in vivo in Tg and wild-type mice (n = 7/group) by delivering 10 brief, high-frequency conditioning stimulus trains (each consisting of 5 pulses, 10 ms duration at 400 Hz). Stimulus pulses were 0.1 ms duration with intensity adjusted to give 20–30% maximal PS amplitude. PS amplitude and latency and pEPSP slope/amplitude were measured simultaneously online for at least 60 min.

Behavioral tests

Behavioral testing was performed using 11 male mice (n = 5 transgenic; n = 6 wild-type) and 14 female mice (n = 7 transgenic; n = 7 wild-type) aged 13 weeks. A within-subject design was employed such that each mouse was subjected to testing in the following order: locomotor activity, light/dark transfer, visual cliff, and Barnes maze, separated by 3–14 days. Mice were group housed under reverse light conditions and all testing was performed during the dark phase of the circadian cycle.

Locomotor activity test

Locomotor activity was measured in Plexiglas cages (42 × 22 × 20 cm) placed into frames (25.5 × 47 cm) mounted with two levels of photocell beams at 2 and 7 cm above the bottom of the cage (San Diego Instruments, San Diego, CA). These two sets of beams allowed for the recording of both horizontal (locomotion) and vertical (rearing) behavior. Mice were placed in the activity boxes for two h.

Light/dark transfer test

The light/dark transfer test takes advantage of the natural conflict of a rodent between the exploration of a novel environment and the aversive properties of a large, brightly-lit open field (Crawley et al., 1997). A greater amount of time in the light compartment and a greater number of transitions are indicative of decreased anxiety-like behavior. The test apparatus is a rectangular box made of Plexiglas divided by a partition into two environments. One compartment (14.5 × 27 × 26.5 cm) is dark (15–25 lx) and the other compartment (28.5 × 27 × 26.5 cm) is highly illuminated (1000–1100 lx) by a 60 W light source located above it. The compartments are connected by an opening (7.5 × 7.5 cm) located at floor level in the center of the partition. The mice were placed in the dark compartment to initiate the test session. Behavior was recorded using a camera mounted above the apparatus. The time spent in each compartment and the number of transitions between compartments were measured. All 4 paws were required to be in a compartment for it to be counted. Each mouse was tested in a single 5-min session.

Visual cliff test

The visual cliff test provides a measure of visual acuity. It evaluates the ability of the animal to see a drop-off at the edge of a horizontal surface (Crawley et al., 1997). In this apparatus, there is the visual appearance of a cliff, but in fact the Plexiglas provides a solid horizontal surface. If the animal sees the cliff, it will step down onto the "safe" side (the horizontal checkered surface) in most trials. A blind animal will just as often step down onto the "negative" side (the vertical appearing surface), i.e., make 50% correct and 50% incorrect choices. Each mouse was placed onto the center ridge, and the side onto which the animal stepped down was recorded. Six consecutive trials were used for each mouse and the percent of correct choices was calculated for each mouse.

Barnes maze

The Barnes maze test is a spatial learning test in which the mouse escapes bright light and noise by entering a tunnel placed under one of 20 holes around the edge of a circular platform g. The Barnes maze used was an opaque Plexiglas disc 75 cm in diameter elevated 58 cm above the floor by a tripod. Twenty holes, 5 cm in diameter, were located 5 cm from the perimeter, and a black Plexiglas escape box (19 × 8 × 7cm) was placed under one of the holes. On the first day of testing, a training session was performed, which consisted of placing a mouse in the escape box and leaving it there for 1 min. One minute later, the first session was started. At the beginning of each session, the mouse was placed in the middle of the maze in a 10-cm high cylindrical black start chamber. After 10 s, the start chamber was removed, a buzzer (80 dB) was turned on, and the mouse set free to explore the maze. The session ended when the mouse entered the escape tunnel or after 5 min elapsed. When the mouse entered the escape tunnel, the buzzer was turned off and the mouse was allowed to remain in the dark for 1 min. In

this spatial version of the task, the tunnel was always located underneath the same hole, which was randomly determined for each mouse. Mice were tested once a day for 40 days or until they met a criterion consisting of three errors or less on 7 of 8 consecutive trials. Errors are defined as searching any hole that does not have the tunnel beneath it.

Statistics

Electrophysiological (in vitro and in vivo) and behavioral data were analyzed using an analysis of variance (ANOVA) to determine statistical significance, considered at $P < 0.05$. For LTP in vitro, we measured differences across the last 15 min of trials (45–60 min post-HFT). For short-term potentiation (STP) in vitro, we analyzed 1–5 min following the trains. To measure differences in input–output functions and paired-pulse facilitation between transgenics and wild-types in vitro, we used unpaired *t* test. For electrophysiological studies in vivo, we measured LTP, paired-pulse responses, and input–output functions.

Behavioral data were analyzed separately for male and female mice. Locomotor data were analyzed using ANOVA with the between subject factor genotype and the within subject factor time interval. Student's *t* tests were used to analyze light/dark transfer and visual cliff data. χ^2 analyses were performed on the Barnes maze data in order to compare the genotypes with regard to meeting the learning criterion for this task on the final day of testing.

Acknowledgments

This work was supported in part by grants from NIH (MH58543 to LdL, NS38633 to MKT, DA08301 to SJH, MH44346 to GRS).

References

Aigner, T.G., 1995. Pharmacology of memory: cholinergic–glutamatergic interactions. Curr. Opin. Neurobiol. 5, 155–160.

Anwyl, R., Lee, W.L., Rowan, M., 1988. The role of calcium in short-term potentiation in the rat hippocampal slice. Brain Res. 459, 192–195.

Baraban, S.C., Tallent, M.K., 2004. Interneuron diversity series: interneuronal neuropeptides—Endogenous regulators of neuronal excitability. Trends Neurosci. 27, 135–142.

Baratta, M.V., Lamp, T., Tallent, M.K., 2002. Somatostatin depresses long-term potentiation and Ca2+ signaling in mouse dentate gyrus. J. Neurophysiol. 88, 3078–3086.

Crawley, J.N., Belknap, J.K., Collins, A., Crabbe, J.C., Frankel, W., Henderson, N., Hitzemann, R.J., Maxson, S.C., Miner, L.L., Silva, A.J., Wehner, J.M., Wynshaw-Boris, A., Paylor, R., 1997. Behavioral phenotypes of inbred mouse strains: implications and recommendations for molecular studies. Psychopharmacology (Berl.) 132, 107–124.

Criado, J., Li, H., Liapakis, G., Spina, M., Henriksen, S., Koob, G., Reisine, T., Sutcliffe, J., Goodman, M., de Lecea, L., 1999. Structural and compositional determinants of cortistatin activity. J. Neurosci. Res. 56, 611–619.

Davis, S., Butcher, S.P., Morris, R.G., 1992. The NMDA receptor antagonist D-2-amino-5-phosphonopentanoate (D-AP5) impairs spatial learning and LTP in vivo at intracerebral concentrations comparable to those that block LTP in vitro. J. Neurosci. 12, 21–34.

de Lecea, L., Criado, J.R., Prospero-Garcia, O., Gautvik, K.M., Schweitzer, P., Danielson, P.E., Dunlop, C.L., Siggins, G.R., Henriksen, S.J., Sutcliffe, J.G., 1996. A cortical neuropeptide with neuronal depressant and sleep-modulating properties. Nature 381, 242–245.

de Lecea, L., del Rio, J.A., Criado, J.R., Alcantara, S., Morales, M., Henriksen, S.J., Soriano, E., Sutcliffe, J.G., 1997a. Cortistatin is expressed in a distinct subset of cortical interneurons. J. Neurosci. 17, 5868–5880.

de Lecea, L., Ruiz-Lozano, P., Danielson, P., Foye, P., Peelle-Kirley, J., Frankel, W., Sutcliffe, J.G., 1997b. cDNA cloning, mRNA distribution and chromosomal mapping of mouse and human preprocortistatin. Genomics 42, 499–506.

Flood, J.F., Uezu, K., Morley, J.E., 1997. The cortical neuropeptide, cortistatin-14, impairs post-training memory processing. Brain Res. 775, 250–252.

Forss-Petter, S., Danielson, P.E., Catsicas, S., Battenberg, E., Price, J., Nerenberg, M., Sutcliffe, J.G., 1990. Transgenic mice expressing beta-galactosidase in mature neurons under neuron-specific enolase promoter control. Neuron 5, 187–197.

Frank, M.G., Issa, N.P., Stryker, M.P., 2001. Sleep enhances plasticity in the developing visual cortex. Neuron 30, 275–287.

Franklin, K.B.J., Paxinos, G., 1997. The Mouse Brain in Stereotaxic Coordinates. Academic Press, New York.

Frazier, C.J., Strowbridge, B.W., Papke, R.L., 2003. Nicotinic receptors on local circuit neurons in dentate gyrus: a potential role in regulation of granule cell excitability. J. Neurophysiol. 89, 3018–3028.

Fukusumi, S., Kitada, C., Takekawa, S., Kizawa, H., Sakamoto, J., Miyamoto, M., Hinuma, S., Kitano, K., Fujino, M., 1997. Identification and characterization of a novel human cortistatin-like peptide. Biochem. Biophys. Res. Commun. 232, 157–163.

Gais, S., Born, J., 2004. Low acetylcholine during slow-wave sleep is critical for declarative memory consolidation. Proc. Natl. Acad. Sci. U. S. A. 101, 2140–2144.

Hasselmo, M.E., 1999. Neuromodulation: acetylcholine and memory consolidation. Trends Cogn. Sci. 3, 351–359.

Hasselmo, M.E., Barkai, E., 1995. Cholinergic modulation of activity-dependent synaptic plasticity in the piriform cortex and associative memory function in a network biophysical simulation. J. Neurosci. 15, 6592–6604.

Jones, S., Yakel, J.L., 1997. Functional nicotinic ACh receptors on interneurones in the rat hippocampus. J. Physiol. 504 (Pt. 3), 603–610.

Klausberger, T., Magill, P.J., Marton, L.F., Roberts, J.D., Cobden, P.M., Buzsaki, G., Somogyi, P., 2003. Brain-state- and cell-type-specific firing of hippocampal interneurons in vivo. Nature 421, 844–848.

Lawrence, J.J., Grinspan, Z.M., Statland, J.M., McBain, C.J., 2003. Differential effects of muscarinic activation on temporal integration in hippocampal oriens/alveus interneurons. Abstract Viewer/Itinerary Planner. Society for Neuroscience: Program, Washington, DC, pp. 799.798.

Leonard, B.J., McNaughton, B.L., Barnes, C.A., 1987. Suppression of hippocampal synaptic plasticity during slow-wave sleep. Brain Res. 425, 174–177.

Louie, K., Wilson, M.A., 2001. Temporally structured replay of awake hippocampal ensemble activity during rapid eye movement sleep. Neuron 29, 145–156.

Malenka, R.C., 1991. Postsynaptic factors control the duration of synaptic enhancement in area CA1 of the hippocampus. Neuron 6, 53–60.

Manabe, T., Noda, Y., Mamiya, T., Katagiri, H., Houtani, T., Nishi, M., Noda, T., Takahashi, T., Sugimoto, T., Nabeshima, T., Takeshima, H., 1998. Facilitation of long-term potentiation and memory in mice lacking nociceptin receptors. Nature 394, 577–581.

Mancillas, J.R., Siggins, G.R., Bloom, F.E., 1986. Somatostatin selectively enhances acetylcholine-induced excitations in rat hippocampus and cortex. Proc. Natl. Acad. Sci. U. S. A. 83, 7518–7521.

McGuinness, N., Anwyl, R., Rowan, M., 1991. The effects of external calcium on the *N*-methyl-D-aspartate induced short-term potentiation in the rat hippocampal slice. Neurosci. Lett. 131, 13–16.

Moore, S.D., Madamba, S.G., Joels, M., Siggins, G.R., 1988. Somatos-

tatin augments the M-current in hippocampal neurons. Science 239, 278–280.

Morris, R.G., Anderson, E., Lynch, G.S., Baudry, M., 1986. Selective impairment of learning and blockade of long-term potentiation by an *N*-methyl-D-aspartate receptor antagonist, AP5. Nature 319, 774–776.

Moser, E.I., Krobert, K.A., Moser, M.B., Morris, R.G.M., 1998. Impaired spatial learning after saturation of long-term potentiation. Science 281, 2038–2042.

Nakao, K., Ikegaya, Y., Yamada, M.K., Nishiyama, N., Matsuki, N., 2001. Spatial performance correlates with long-term potentiation of the dentate gyrus but not of the CA1 region in rats with fimbria-fornix lesions. Neurosci. Lett. 307, 159–162.

Paxinos, G., Watson, A., 1986. The Rat Brain: An Stereotaxic Atlas. Academic Press, San Diego.

Qiu, C., Suntheimer, R.J., Tallent, M.K., 2003. Somatostatin depresses CA1 long term potentiation. Abstract Viewer/Itinerary Planner. Society for Neuroscience: Program, Washington, DC, pp. 889.881.

Robas, N., Mead, E., Fidock, M., 2003. MrgX2 is a high potency cortistatin receptor expressed in dorsal root ganglion. J. Biol. Chem. 278, 44400–44404.

Rosenzweig, E.S., Barnes, C.A., 2003. Impact of aging on hippocampal function: plasticity, network dynamics, and cognition. Prog. Neurobiol. 69, 143–179.

Sakimura, K., Kutsuwada, T., Ito, I., Manabe, T., Takayama, C., Kushiya, E., Yagi, T., Aizawa, S., Inoue, Y., Sugiyama, H., et al., 1995. Reduced hippocampal LTP and spatial learning in mice lacking NMDA receptor epsilon 1 subunit. Nature 373, 151–155.

Sanchez-Alavez, M., Gomez-Chavarin, M., Navarro, L., Jimenez-Anguiano, A., Murillo-Rodriguez, E., Prado-Alcala, R.A., Drucker-Colin, R., Prospero-Garcia, O., 2000. Cortistatin modulates memory processes in rats. Brain Res. 858, 78–83.

Schweitzer, P., Madamba, S.G., Siggins, G.R., 2003. The sleep-modulating peptide cortistatin augments the h-current in hippocampal neurons. J. Neurosci. 23, 10884–10891.

Siehler, S., Seuwen, K., Hoyer, D., 1998. [125I]Tyr10-cortistatin14 labels all five somatostatin receptors. Naunyn Schmiedebergs Arch. Pharmacol. 357, 483–489.

Spier, A.D., Fabre, V., de Lecea, L., 2005. Cortistatin radioligand binding in wild-type and somatostatin receptor-deficient mouse brain. Regul. Pept. 124, 179–186.

Sun, Q.Q., Baraban, S.C., Prince, D.A., Huguenard, J.R., 2003. Target-specific neuropeptide Y-ergic synaptic inhibition and its network consequences within the mammalian thalamus. J. Neurosci. 23, 9639–9649.

Tsien, J.Z., Huerta, P.T., Tonegawa, S., 1996. The essential role of hippocampal CA1 NMDA receptor-dependent synaptic plasticity in spatial memory. Cell 87, 1327–1338.

Videau, C., Hochgeschwender, U., Kreienkamp, H.J., Brennan, M.B., Viollet, C., Richter, D., Epelbaum, J., 2003. Characterisation of [125I]-Tyr0DTrp8-somatostatin binding in sst1- to sst4- and SRIF-gene-invalidated mouse brain. Naunyn Schmiedeberg's Arch. Pharmacol. 367, 562–571.

Wilson, M.A., McNaughton, B.L., 1994. Reactivation of hippocampal ensemble memories during sleep. Science 265, 676–679.

Winsky-Sommerer, R., Spier, A.D., Fabre, V., de Lecea, L., Criado, J.R., 2004. Overexpression of the human beta-amyloid precursor protein down-regulates cortistatin mRNA in PDAPP mice. Brain Res. 1023, 157–162.

Yu, T.P., Xie, C.W., 1998. Orphanin FQ/nociceptin inhibits synaptic transmission and long-term potentiation in rat dentate gyrus through postsynaptic mechanisms. J. Neurophysiol. 80, 1277–1284.